

## Scattering of Protons by Helium between 11.4 Mev and 18 Mev\*

KARL W. BROCKMAN†

*Palmer Physical Laboratory, Princeton University, Princeton, New Jersey*

(Received August 6, 1957)

Measurements of the elastic differential cross section for the scattering of protons by helium have been made at 12 energies between 11.4 Mev and 18 Mev. Ten scattering angles were used spaced at 15° intervals from 30° to 165° in the laboratory system; however, not all the angles were used at each energy. Standard gas-scattering techniques were employed. Scattered particles were detected by a scintillation counter and recorded on a 20-channel pulse-height analyzer. At nine of the scattering angles (165° excluded), smoothed curves of the cross section *versus* energy were plotted and values taken from these curves were analyzed in terms of *S*- and *P*-wave phase shifts. Two separate sets of *S* and *P* phase shifts intersecting at about 13 Mev were found. Least-squares fits are given for the solutions which are a continuation of phase-shift analyses at lower energies. Attempts to include *D* waves in the fits failed. There is evidence that *D* phase shifts remain less than about 8° up to 16 Mev; however, at 18 Mev it appears that some *D* wave may be required. Rough agreement with current polarization experiments is cited.

### I. INTRODUCTION

MEASUREMENTS of the differential cross section for the scattering of protons by helium have been made numerous times since 1949 in the energy range between 0.95 and 9.74 Mev.<sup>1-8</sup> The results have been analyzed in terms of phase shifts<sup>9-11</sup> and these in turn have been discussed theoretically in several papers.<sup>12-16</sup>

Last year the author published a cross section taken at 17.45 Mev<sup>17</sup> along with a set of phase shifts that almost fit the data but otherwise seemed unsatisfactory. The experiments described in the present paper were undertaken to bridge the gap between 17.45 Mev and the lower energy work with the hope of being able to follow the phase shifts up in energy without recourse to any model for the interaction.

### II. EXPERIMENTAL PROCEDURE

In a departure from the previous procedure of measuring the cross section of many angles at a fixed energy, the procedure here was to use a limited number of angles, which remained fixed, at several energies.

Figure 1 shows the scattering chamber and the arrangement used for observing scattering from a gas target. The chamber is 12 inches in diameter and has cylindrical ports 1½ inches in diameter extending 2 inches beyond the chamber walls through which scattering is observed. On one side of the chamber ports are at angles of 30°, 60°, 90°, 120° and 150°, and on the other side the angles are 12°, 45°, 75°, 105°, 135°, and 165°; the 12° port, however, was not used for cross section measurements.

The usual practice in gas scattering is to define the thickness of the target and the solid angle subtended by the detector by a pair of slits in front of the detector. In this experiment these slits were mounted in a set of tubes that were plugged into the ports on the scattering chamber. The slit closest to the center of the chamber is a vertical rectangular opening of sufficient height that every point on the slit at the rear of the tube can see the full vertical extent of the proton beam passing through the chamber. This forward slit was placed so that it was flush with the wall of the chamber, that is, at a distance of about 6 inches from the scattering center. The rear slit was a circular hole placed at a distance of 6 to 8 inches beyond the rectangular one. Sizes of the slits and the distances between them varied from angle to angle, the particular dimensions being chosen to obtain a reasonable counting rate at all angles. The width of the rectangular slit and the diameter of the circular hole were approximately equal for each angle, ranging from  $\frac{5}{16}$  inch with 8 inches between slits for 30° where the counting rate was highest to  $\frac{5}{8}$  inch with 6 inches between slits at 90° and 105° where the counting rate was lowest. The same combinations of slits were used at all energies. Slit dimensions were measured with a traveling microscope and the distances of the slits from the center of the chamber for the different angles were found using a variety of micrometers and precision vernier calipers. It is estimated that uncertainties in these dimensions contribute less than 0.1% to the uncertainties in the values obtained for the cross section

At a scattering angle  $\theta$ , the product of the thickness

\* This work was supported by the U. S. Atomic Energy Commission and the Higgins Scientific Trust Fund.

† Now at Instituut voor Kernfysisch Onderzoek, Amsterdam, The Netherlands.

<sup>1</sup> Freier, Lampi, Sleator, and Williams, *Phys. Rev.* **75**, 1345 (1949).

<sup>2</sup> C. H. Braden, *Phys. Rev.* **84**, 762 (1951).

<sup>3</sup> T. M. Putnam, *Phys. Rev.* **87**, 932 (1952).

<sup>4</sup> Kreger, Jentschke, and Kruger, *Phys. Rev.* **93**, 837 (1954).

<sup>5</sup> Freemantle, Grottdal, Gibson, McKeague, Prowse, and Rotblat, *Phil. Mag.* **45**, 1090 (1954).

<sup>6</sup> B. Cork and W. Hartsough, *Phys. Rev.* **96**, 1267 (1954).

<sup>7</sup> J. H. Williams and S. W. Rasmussen, *Phys. Rev.* **98**, 56 (1955).

<sup>8</sup> Putnam, Brolley, and Rosen, *Phys. Rev.* **104**, 1303 (1956).

<sup>9</sup> C. L. Critchfield and D. C. Dodder, *Phys. Rev.* **76**, 602 (1949).

<sup>10</sup> D. C. Dodder and J. L. Gammel, *Phys. Rev.* **88**, 520 (1952).

<sup>11</sup> H. Lustig and J. M. Blatt, *Phys. Rev.* **100**, 777 (1955).

<sup>12</sup> R. D. Adair, *Phys. Rev.* **86**, 155 (1952).

<sup>13</sup> Sack, Biedenharn, and Breit, *Phys. Rev.* **93**, 321 (1954).

<sup>14</sup> Hochberg, Massey, and Underhill, *Proc. Phys. Soc. (London)* **A67**, 957 (1954).

<sup>15</sup> Hochberg, Massey, Robertson, and Underhill, *Proc. Phys. Soc. (London)* **A68**, 746 (1955).

<sup>16</sup> E. van der Spuy, *Nuclear Phys.* **1**, 381 (1956).

<sup>17</sup> K. W. Brockman, *Phys. Rev.* **102**, 391 (1956).

of the gas target and the solid angle subtended by the detector as determined by the slit geometry is given approximately by  $(Ad/Rl) \csc\theta$ , with  $A$  the area of the circular hole,  $d$  the width of the vertical slit,  $l$  the distance between slits, and  $R$  the distance from the circular hole to the center of the chamber. Corrections to the cross section as calculated with this formula, due to the finite geometry and to the slope and curvature of the cross section with respect to the scattering angle, have been discussed in a paper by Critchfield and Dodder.<sup>18</sup> These corrections were applied, but in no case did they exceed 0.3%

The tubes carrying the slits were mounted in the ports on the scattering chamber on a pair of O rings spaced  $1\frac{3}{8}$  inches apart in grooves on the outer surface of the tubes. A ledge on the tubes provided radial positioning; under the partial vacuum in the chamber, the ledges butted firmly against the ends of the ports. This arrangement was such that the same geometric situation could be reproduced accurately on different occasions by merely plugging in the tubes. Scattering angles were determined by measuring the angle between a mandrel similarly mounted in one of the ports and a mandrel through the incident-beam collimation slits with a precision protractor. Errors in these measurements did not exceed  $\pm 5$  minutes of arc.

Collimation of the incident beam was accomplished with two circular holes  $\frac{1}{4}$  inch in diameter and  $12\frac{1}{2}$  inches apart along the beam tube from the cyclotron, and attached to the scattering chamber with the axis of the holes crossing the center of the chamber. The chamber and collimators were placed so that the axis of collimation coincided with the line of maximum beam from the machine. A 2-mil aluminum foil over the collimator nearest the cyclotron sealed the gas in the chamber from the vacuum in the beam tube and served to spread the beam over the area of the second collimator. To obtain measurements at energies below 15 Mev, additional polystyrene foils were added to this point to moderate the beam energy. A second 2-mil aluminum foil was placed about a foot farther up the beam tube to spread the beam and assure uniform illumination of the foils over the first collimator. Failure of the beam to be parallel with the axis of collimation would lead to a systematic error in all measurements; however, with the precautions taken it is felt that an error in scattering angles no greater than 7 minutes of arc resulted from this effect. An error of angle of this order would cause an error in the reported cross sections of about 0.3% in the worst case.

Scattered protons were detected in a sodium iodide scintillation counter, and the pulses were recorded on an Atomic Instruments 20-channel differential pulse-height analyzer. At large scattering angles, where the energy of scattered protons is low, it was necessary to subtract background pulses due mainly to 4.4-Mev

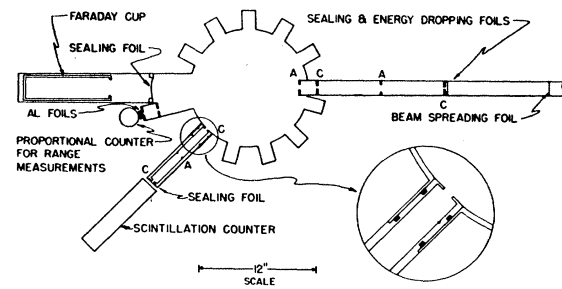


FIG. 1. Schematic diagram of scattering chamber, showing setup for scattering at  $45^\circ$  and beam-energy measurement. Detail shows O-ring mounting of analyzing slit tubes. Slits labeled C are collimators, those labeled A are anticattering slits.

gamma rays from graphite collimators. This was done by placing enough aluminum just in front of the counter to stop protons completely, then observing the background spectrum alone. At the lower bombarding energies, it was not always possible to perform this subtraction with the desired accuracy, and consequently measurements at some of the largest angles were abandoned. Statistical errors in counting, including background subtraction, amount to between 1% and 2.3% for all measurements.

Commercial helium gas (refined for welding) proved to be of sufficient purity for the experiment, and no further purification was attempted. Cleanness of the proton spectrum at energies where elastic scattering by impurities would occur indicated that fewer than 0.1% of the recorded pulses were due to impurities. The density of the gas was found by measuring the temperature and pressure of the sample in the chamber. Pressures ranging between 25 and 30 cm of mercury were measured with a mercury manometer, and the temperature was taken to be that of a thermometer laid on the lid of the scattering chamber. Negligible error is likely to have occurred in this procedure since the temperature of the room itself was stable within a few tenths of a centigrade degree. Pressure and temperature measurements were usually recorded after the gas had remained in the chamber about half an hour.

Integration of the incident proton current was done by catching the beam in a Faraday cup and measuring the voltage developed across a calibrated polystyrene capacitor attached to the cup with a quadrant electrometer. Calibration of the capacitor was by the National Bureau of Standards and that of the electrometer was determined with a standard cell. The chamber containing the Faraday cup was sealed from the scattering chamber with a 2-mil aluminum foil and evacuated to a pressure of around  $10^{-5}$  mm of mercury. The length of a particular run was set by the requirement that the voltage on the cup be no greater than 0.7 volt. Because of this several runs were required at the slower angles to obtain the desired statistics. Sensitivity of the integration to the voltage on the cup was investigated by biasing the cup positive and negative and

<sup>18</sup> C. L. Critchfield and D. C. Dodder, Phys. Rev. **75**, 419 (1949).

TABLE I. Center-of-mass proton-helium differential scattering cross section in millibarns per steradian and estimated percent error as a function of center-of-mass scattering angle and laboratory energy. Proton energies are in Mev.

$\frac{E_p}{\theta}$	11.42	11.65	12.49	12.58	13.30	13.65	14.38	14.49	15.05	16.24	16.76	17.84
36.72°	264.2 ± 2.1%	260.6 ± 2.1%	242.1 ± 1.9%	163.2 ± 1.8%	236.2 ± 2.0%		220.0 ± 1.9%		217.2 ± 1.9%	195.9 ± 2.0%	189.8 ± 1.9%	176.3 ± 2.0%
55.55°	180.2 ± 1.9%	165.9 ± 2.0%			154.1 ± 1.9%		142.7 ± 1.9%		139.1 ± 1.8%	126.6 ± 1.8%	122.9 ± 1.6%	115.6 ± 1.7%
72.03°	101.9 ± 1.8%	98.5 ± 1.9%	91.6 ± 1.8%		89.3 ± 1.8%		82.3 ± 1.8%		81.2 ± 1.7%	72.9 ± 1.8%	69.1 ± 1.9%	63.7 ± 1.8%
89.60°	43.5 ± 1.9%	41.6 ± 1.9%	38.2 ± 1.9%		35.7 ± 1.8%		33.3 ± 1.8%		32.1 ± 1.9%	28.27 ± 1.9%	27.85 ± 2.0%	26.08 ± 1.9%
104.83°		18.43 ± 2.1%	15.86 ± 2.3%		14.76 ± 2.0%		13.17 ± 2.0%		12.78 ± 2.1%	10.92 ± 2.2%	10.50 ± 2.1%	9.54 ± 2.1%
119.07°		15.95 ± 2.0%		14.43 ± 2.1%	13.06 ± 1.9%		11.25 ± 2.1%		11.21 ± 2.2%	9.36 ± 2.1%	8.99 ± 1.9%	8.29 ± 2.0%
132.02°		27.30 ± 2.2%	24.60 ± 2.4%		22.71 ± 1.9%		21.02 ± 1.9%		20.34 ± 1.9%	18.12 ± 2.0%	16.90 ± 1.9%	15.97 ± 2.0%
145.25°			41.3 ± 2.5%		40.4 ± 2.4%		37.4 ± 2.3%		37.0 ± 2.4%	32.2 ± 2.1%	30.5 ± 2.2%	28.62 ± 2.1%
156.87°					57.0 ± 3.1%		50.4 ± 1.9%	50.2 ± 2.2%	49.4 ± 2.6%	44.7 ± 2.3%	42.3 ± 2.3%	38.7 ± 2.2%
169.05°						53.7 ± 2.3%			57.7 ± 2.9%	52.1 ± 2.6%	49.6 ± 2.8%	45.4 ± 2.7%

observing the charge collected *versus* the number of protons scattered by a target into a monitor counter. During cross section measurements no secondary-electron suppression device was used, because it would have made measurements at some angles awkward. A correction to the data was determined, however, in subsequent monitored runs using a large alnico permanent magnet with which a field of 500 to 1000 gauss could be put across wide regions of the cup. The results of these investigations indicated that a systematic error in the integration amounted to less than 0.5%. Random errors in reading the electrometer were no greater than 0.3%.

Proton beams of good intensity can be obtained from the Princeton FM cyclotron with energies between 15 and 19 Mev. To obtain lower energies, it was necessary to insert foils at the previously mentioned location to slow down the protons. In such an operation, a spread is introduced in the proton energies in the beam which can lead to erroneous cross section measurements. However, the spread may be calculated from energy loss theory and the variation of the cross section with energy was known at each angle, so that a correction could be calculated for this effect. The correction proved to be less than 0.2% for the worst case. Skewness of the distribution of proton energies may also lead to errors, but in this case the difference between the mean energy and the most probable energy in the distribution was less than half the uncertainty of the energy measurements, and no corrections were considered.

The energy of the incident beam was found by measuring the range in aluminum of protons scattered through the 12° port of the chamber by the target gas. Measured aluminum foils were inserted in front of a thin argon-filled proportional counter and integral range curves were determined. Ranges were converted to energies using the range-energy relations of Bichsel, Mozley, and Aron.<sup>19</sup> With this method, the mean incident energy of the beam could be found within 50 keV; errors in the measurements probably did not exceed this value. The energy spread in the beam of the Princeton cyclotron is about 250-keV full width at half maximum being roughly Gaussian in shape.<sup>20</sup> The effect of this spread was considered with the corrections mentioned in the preceding paragraph. Measurements of the energy were made three or four times during the course of an experiment at a particular energy. It was found that the energy remained stable within ±50 keV during the course of experiments if the cyclotron was allowed to run about two hours before measurements were begun. All measurements listed for a particular energy were made after this stabilization period, and were completed before the cyclotron was shut off. The energies reported may therefore be considered to be accurate within ±100 keV.

<sup>19</sup> Bichsel, Mozley, and Aron, Phys. Rev. **105**, 1788 (1957).

<sup>20</sup> G. Schrank, Rev. Sci. Instr. **26**, 677 (1955).

The differential cross sections measured are listed in Table I together with the estimated probable errors. Center-of-mass cross sections and angles are given. Relativistic corrections were applied to the classical center-of-mass transformations; however, at these energies they were hardly necessary, being of the order of 0.5% and less. The over-all absolute accuracy of the experiment is estimated to be between  $\pm 2\%$  and  $\pm 3\%$ .

For the purpose of comparing these cross sections with the work at adjacent energies it is most convenient to use the dimensionless quantity  $k^2\sigma$ ,  $k$  being the wave number of the incident protons and  $\sigma$  the cross section. This takes out most of the energy variation leaving more slowly varying curves at each angle which may be easily extrapolated to observe agreement with the other measurements. The cross sections given here agree fairly well with those at 9.48 Mev<sup>3</sup> and 9.74<sup>7</sup> and with the author's own work at 17.45 Mev. The poorest agreement was at the 36.72° (c.m.) scattering angle where the extrapolated cross section lay about 5% below that reported at 9.48 Mev. This is within the sum of the reported probable errors for the experiments, however. At other angles the agreement seemed much better. With regard to the 17.45-Mev data, it should be stated that that cross section may be considered entirely independent of those reported in this paper since no apparatus, except the cyclotron, was common to the two sets of measurements.

In the analysis of the data discussed below, the reported cross sections themselves were not used, but rather graphs of  $k^2\sigma$  versus energy were plotted for each scattering angle, and values were taken from smooth curves drawn through the experimental points. Doing this served to smooth out random fluctuations in the measured values and allowed attention to be paid to the independent experiments at adjacent energies. Once such curves are drawn, there is no longer any reason to perform the analyses at the energy values at which the measurements were made; thus, in the work described in the following section, integral values of the energy in Mev were used.

### III. PHASE SHIFTS

In proton-helium scattering, states of different total angular momentum, but with the same orbital angular momentum, scatter differently because of spin-orbit interaction. Thus, in an analysis of scattering data one expects to find one  $S$  phase shift,  $\delta_0$ , two  $P$  phase shifts, the  $P_{\frac{3}{2}}$  phase shift,  $\delta_{1+}$ , and the  $P_{\frac{1}{2}}$  phase shift,  $\delta_{1-}$ , which are, respectively, the phase shifts for partial waves with total angular momentum  $\frac{3}{2}$  and  $\frac{1}{2}$ , two  $D$  phase shifts,  $\delta_{2+}$  for the  $D_{\frac{5}{2}}$  wave and  $\delta_{2-}$  for the  $D_{\frac{3}{2}}$  wave, and so on, the number of partial waves contributing significantly to the scattering depending on the energy of bombardment. In the energy range covered in these experiments it seems likely that  $D$ -wave scattering should become important. Phase-shift

analyses of the data below 9.5 Mev<sup>8,10</sup> indicate  $D$  phase shifts of the order of a few degrees, and it may be expected that these remain small at least at the lower energies of the present experiment. On this basis, the procedure was first to fit the data as well as possible with  $S$  and  $P$  waves and then to investigate inclusion of  $D$  waves.

Preliminary solutions with  $S$  and  $P$  waves were made following the procedure outlined by Critchfield and Dodder<sup>9</sup> in which the expression for the cross section in terms of the phase shifts is equated to the experimental values of the cross section at the angles 54°44', 125°16', and 90°, and the three equations are solved for the three phase shifts. This method has the advantage of not only finding initial values with which to start a least-squares fitting procedure, but also maps out the alternative solutions which fit the data but are not physically significant. Solutions were found using values taken from the  $k^2\sigma$  graphs mentioned above at 12, 14, and 16 Mev, and were also found for the 5.78-Mev data<sup>4</sup> and the 9.48-Mev data<sup>3</sup> to establish continuity of sets of solutions.

The angles 54°44' and 90° are sufficiently close to two of the angles where measurements were made to make extrapolation of the values of  $k^2\sigma$  along the angular distributions from the measured angle to the angle used in the calculation reliable; however, the angle 125°16' is almost midway between the angles 119.07° and 132.02° where measurements were made. For 125°16',  $k^2\sigma$  was interpolated between the values at these two angles under the assumption that the shape of the angular distribution in this region is about the same as at 17.45 Mev and 9.48 Mev where more complete experimental angular distributions are available. Justification for this procedure is in fact that  $S$ - and  $P$ -wave phase shifts found this way agreed with those found for least-squares fits to all the measured points.

In the procedure of Critchfield and Dodder, a trial  $S$  phase shift,  $\delta_0$ , is chosen, introduced into the equations for the cross section at 54°44' and 125°16', and this pair of equations is solved for a pair of parameters,  $\beta$  and  $\rho$ , related to the  $P$  phase shifts  $\delta_{1+}$  and  $\delta_{1-}$ . These two values are then introduced into the 90° equation and this is solved for the  $S$  phase shift. The procedure is repeated with a number of trial  $\delta_0$ 's for each of which a calculated  $\delta_0$  is obtained, and the solution occurs when the calculated  $\delta_0$  equals the trial  $\delta_0$ . In general, there may be more than one solution. For each such solution the  $P$  phase shifts may be found by solving equations relating them to the parameters  $\beta$  and  $\rho$ . Two sets of  $P$ -wave solutions are found for each  $S$ -wave solution corresponding to the inverted and normal doublet possibilities for the  $P$  states in Li<sup>5</sup>. The polarization experiment of Heusinkveld and Freier<sup>21</sup> established that the inverted doublet solutions are those actually occurring, and in Table II, in which the results

<sup>21</sup> M. Heusinkveld and G. Freier, Phys. Rev. 85, 80 (1952).

TABLE II. Inverted-doublet proton-helium phase shifts obtained by Critchfield and Dodder's three-point method for five energies. Set *A* is the physically significant one.

Energy (Mev)	<i>A</i>			<i>B</i>		
	$\delta_0$	$\delta_{1^+}$	$\delta_{1^-}$	$\delta_0$	$\delta_{1^+}$	$\delta_{1^-}$
5.78	-44.1°	115.7°	40.3°	-77.5°	72.1°	19.4°
9.48	-59.4°	112.1°	58.2°	-71.6°	86.6°	40.4°
12.0	-70.4°	100.4°	54.5°	-70.4°	100.4°	54.5°
14.0	-75.4°	96.7°	53.7°	-71.3°	105.2°	60.5°
16.0	-79.9°	92.4°	52.0°	-70.8°	110.0°	66.9°

of these calculations are given, only the inverted doublet solutions are listed.

In practice it is most convenient to work with Critchfield and Dodder's parameter  $\alpha$  which is closely related to  $\delta_0$  rather than with  $\delta_0$ . Solutions were found by plotting the assumed  $\cos\alpha$  and the calculated  $\cos\alpha$  against the assumed  $\alpha$  and looking for intersections of the two curves (it turns out that for most  $\alpha$ 's the calculated  $|\cos\alpha| > 1$ ). For the energy region investigated, the calculated  $\cos\alpha$  curve is concave away from the  $\alpha$  axis while the assumed  $\cos\alpha$  curve is, of course, concave toward the  $\alpha$  axis, and the two intersect at nearby points. At 9.48 Mev these two points are closer together than at 5.78 Mev, and at 12 Mev there is no intersection at all. However, at 14 Mev there are again two intersections which are in turn wider spaced at 16 Mev. A similar situation occurred at 2.53 Mev in the work of Critchfield and Dodder, and the interpretation here is as there that two sets of solutions intersect, the physically significant  $\alpha$  changing from the larger of the pair to the smaller of the pair. At the actual point of intersection of the two sets of phase shifts, the two  $\cos\alpha$  curves should be tangent. The failure of these curves to touch at 12 Mev is probably due to experimental uncertainties in the measured cross sections; actually at this energy the curves came very close together. It should be remarked that it is also impossible to obtain solutions by using the 9.48-Mev data as it was reported. The solutions given in Table II were found by reducing this cross section by 2½%, which is within the estimated probable error reported for that experiment. If one accepts the conclusion of the present work that the *D* phase shifts remain small up to 18 Mev, he might then conclude that the 9.48-Mev data is systematically high by a percent or two. That the two possible sets of phase shifts do cross over is also borne out in examination of the energy variation of the *P* shifts as well as that of various parameters occurring in the course of the solutions.

The phase shifts calculated by this method are given in Table II, in which only the inverted doublet solutions for *P* phase shifts are listed. Set *A* in the table is the physically significant one which corresponds to Dodder and Gammel's<sup>10</sup> solution *A* at 9.48 Mev and their solution at 5.81 Mev. At 12 Mev, where there was no intersection of the  $\cos\alpha$  curves, the value of  $\alpha$  used was that corresponding to the closest approach of the

two curves to each other. It should be noted that solution *B* at 9.48 Mev is not Dodder and Gammel's solution *C* which occurs at a still different intersection of the  $\cos\alpha$  curves.

Least-squares fits to the data in terms of *S* and *P* waves were found with an IBM 650 data-processing machine by employing an iterative procedure in which the phase shifts were changed from an initial value along the line of maximum gradient of the relative deviations from the experimental data. In this calculation the criterion of convergence of the phase shifts to the values providing a least-squares fit was that the change in all phase shifts from one iteration to the next be less than 0.1°. The data used in the calculation were taken from the  $k^2\sigma$  curves at 12, 13, 14, 15, 16, 17, and 18 Mev. Only nine of the experimental scattering angles were used, measurements at 169.05° being excluded because of the limited number of observations at that angle. The calculation at 12 Mev did not converge but rather oscillated between two nearby values. This behavior is not surprising since it was seen in the above discussion that this energy is at, or near, the crossing of two separate sets of solutions. Random errors in the measurements probably prevent convergence to the one set or the other. At 13 Mev only one solution was found, and at 14 Mev and higher convergence could be obtained to either set *A* or set *B* of the solutions obtained by solving the equations by the Critchfield and Dodder method. This indicates that the cross over of solutions probably occurs closer to 13 Mev than it does to 12 Mev.

The results of these calculations are given in Table III. For each energy the phase shifts<sup>22</sup> providing least-squares fits are given along with the experimental  $k^2\sigma$  values and the percent deviation of the calculated  $k^2\sigma$  values from these. Only the physically relevant phase shifts are given, i.e., those corresponding to set *A*. At 12 Mev the solution given is the closest fit in that branch of the oscillation corresponding to set *A*. It is seen that in general the calculated cross sections differ from the experimental cross sections by values within the estimated experimental probable error except at 12 Mev. The large deviations at that energy are probably due to improper extrapolation of the  $k^2\sigma$  values at 156.87° and 169.05° from the higher energy data. In the over-all picture the fits seem quite good.

Attempts were made to include *D*-wave phase shifts in the least-squares fit. In doing this, no program was written for the situation where the  $D_{3/2}$  and  $D_{5/2}$  phase shifts are locked together, but only for the case where they could take on separate values. This work was not successful, for in almost every case the fitting procedure diverged. A possible explanation for this is that in view of experimental errors, only nine scattering angles do not sufficiently overdetermine a fit in terms

<sup>22</sup> *S* phase shifts are given as negative following the custom of previous work; however, there is reason to believe that the true values are obtained by adding 180°. See references 14 and 16.

TABLE III.  $S$  and  $P$  phase shifts providing least-squares fits to experimental data at several energies. Experimental  $k^2\sigma$  values and percent deviation of cross sections calculated from phase shifts from the experimental cross sections are given as a function of center-of-mass angle and laboratory energy. The rms deviation is included for each energy.

Energy $\theta_{c.m.}$	12 Mev		13 Mev		14 Mev		15 Mev		16 Mev		17 Mev		18 Mev	
	$k^2\sigma$	% dev	$k^2\sigma$	% dev	$k^2\sigma$	% dev	$k^2\sigma$	% dev	$k^2\sigma$	% dev	$k^2\sigma$	% dev	$k^2\sigma$	% dev
	$\delta_0 = -66.9^\circ$		$\delta_0 = -71.4^\circ$		$\delta_0 = -76.7^\circ$		$\delta_0 = -79.0^\circ$		$\delta_0 = -81.1^\circ$		$\delta_0 = -83.4^\circ$		$\delta_0 = -85.8^\circ$	
	$\delta_1^+ = 108.7^\circ$		$\delta_1^+ = 103.0^\circ$		$\delta_1^+ = 92.7^\circ$		$\delta_1^+ = 91.1^\circ$		$\delta_1^+ = 89.5^\circ$		$\delta_1^+ = 87.5^\circ$		$\delta_1^+ = 85.4^\circ$	
	$\delta_1^- = 60.1^\circ$		$\delta_1^- = 57.0^\circ$		$\delta_1^- = 50.2^\circ$		$\delta_1^- = 49.7^\circ$		$\delta_1^- = 49.1^\circ$		$\delta_1^- = 47.9^\circ$		$\delta_1^- = 46.4^\circ$	
36.72°	9.60	-2.08	9.72	-1.48	9.80	0.82	9.85	0.12	9.87	-0.53	9.88	-1.66	9.88	-3.17
55.55°	6.25	-1.63	6.31	-0.05	6.35	0.63	6.37	0.57	6.38	0.31	6.38	-0.26	6.36	-0.95
72.03°	3.638	-3.02	3.668	-1.87	3.680	-1.63	3.670	-1.27	3.636	-0.49	3.575	0.75	3.495	2.26
89.60°	1.504	0.13	1.481	1.30	1.464	1.35	1.445	2.02	1.430	2.30	1.416	2.59	1.410	2.37
104.83°	0.650	-1.08	0.615	-1.22	0.593	-1.72	0.572	-1.78	0.555	-1.77	0.540	-1.41	0.527	-0.57
119.07°	0.572	-0.35	0.545	-0.87	0.518	0.58	0.492	0.68	0.471	0.85	0.454	0.26	0.439	-0.36
132.02°	0.970	-0.41	0.940	2.51	0.933	2.56	0.918	1.43	0.904	0.55	0.875	0.64	0.850	-0.12
145.25°	1.655	-3.32	1.650	-0.88	1.650	-1.30	1.636	-0.88	1.606	-0.45	1.561	0.03	1.502	0.80
156.87°	2.250	-3.98	2.260	-1.68	2.268	-1.75	2.255	-1.38	2.215	-0.63	2.163	-0.27	2.080	0.85
Rms dev.		2.22		1.47		1.50		1.26		1.09		1.19		1.62

of five parameters to prevent excessively large increments in the phase shifts from occurring between successive iterations.

A somewhat different approach to the problem of finding  $D$  phase shifts was made as follows. The set of phase shifts  $(\delta_0, \delta_1^+, \delta_1^-; \delta_2^+, \delta_2^-)$  provides a reasonably good fit to the data when  $\delta_0, \delta_1^+, \delta_1^-$  are those found above and  $\delta_2^+$  and  $\delta_2^-$  are zero. The question now arises whether a set of phase shifts with  $\delta_2^+$  and  $\delta_2^-$  not zero and with different  $S$  and  $P$  phase shifts will fit the data equally well. In energy regions where the  $D$  phase shifts are small, the change in  $\delta_0, \delta_1^+, \delta_1^-$  will also be small. Let this set of phase shifts be denoted by  $(\delta_0 + \Delta\delta_0, \delta_1^+ + \Delta\delta_1^+, \delta_1^- + \Delta\delta_1^-, \Delta\delta_2^+, \Delta\delta_2^-)$ . Using a linear approximation, a condition that must be satisfied for equally good fits of the two sets of phase shifts is that the expression,

$$\frac{\partial\sigma}{\partial\delta_0}\Delta\delta_0 + \frac{\partial\sigma}{\partial\delta_1^+}\Delta\delta_1^+ + \frac{\partial\sigma}{\partial\delta_1^-}\Delta\delta_1^- + \frac{\partial\sigma}{\partial\delta_2^+}\Delta\delta_2^+ + \frac{\partial\sigma}{\partial\delta_2^-}\Delta\delta_2^-,$$

be zero or very small for each of the data points. In this expression,  $\sigma$  is the cross section and the derivatives are evaluated at the initial point  $(\delta_0, \delta_1^+, \delta_1^-, 0, 0)$ . Expressions of this type were examined closely at 13 Mev and 16 Mev to determine what departure from the  $S$ - and  $P$ -wave fits could be made to include  $D$ -wave effects. Only a very few departures looked remotely possible at all, and those that looked fair at the one energy looked poor at the other. These served as starting points for five-parameter least-squares fits, but in every case there was divergence. At both of these energies it was never possible to change any phase shift by more than eight or ten degrees and making the best possible compensating shift with the rest of the phase shifts without ruining the three-parameter fits. The conclusion drawn from these investigations is that either the  $D$  phase shifts remain small (less than about  $8^\circ$ ) throughout the energy region, or that the  $D$ -wave departure occurs at lower energies and that second and high order terms contribute to the above expression in

such a way as to allow equally good three- and five-parameter fits. This latter possibility seems unlikely especially in view of the good three-parameter fits which, moreover, agreed with the solutions obtained with the three-point Critchfield and Dodder method.

A graph of the  $S$  and  $P$  phase shifts, including those at lower energies, is shown in Fig. 2. In this graph the negative of the  $S$  phase shift is plotted. The lines drawn through the points have no significance. The values plotted would appear to be good to within  $\pm 7^\circ$ , which is about the amount any particular phase shift may be changed with compensating changes in the others without destroying the fit. Reservations to this statement are to be made.

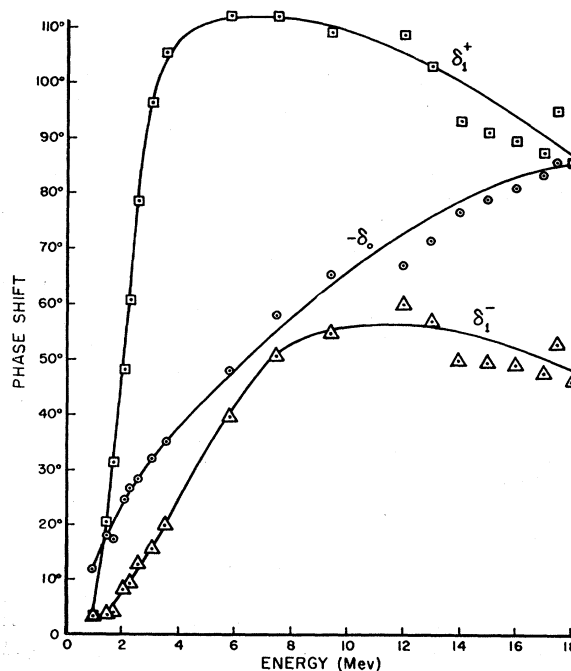


FIG. 2.  $S$  and  $P$  phase shifts resulting from least-squares analyses versus laboratory energy. Points below 10 Mev are taken from references 8, 9, and 10.

TABLE IV. Experimental and calculated cross sections for the 17.45-Mev data.

$\theta_{c.m.}$ (degrees)	$\sigma_{c.m.}$ experimental (mb/sterad)	I		II	
		$\sigma_{c.m.}$ calculated (mb/sterad)	% deviation	$\sigma_{c.m.}$ calculated (mb/sterad)	% deviation
6.38	2510	2263	-9.8	2394	-4.6
7.62	1200	1106	-7.8	1198	-0.2
8.87	700	632	-9.7	702	0.3
10.11	475	420	-11.5	476	0.2
11.36	365	316	-13.4	363	-0.5
12.60	308	263	-14.5	303	-1.6
15.08	253	220	-13.0	250	-1.2
17.56	235	206	-12.3	230	-3.4
21.28	225	199	-11.5	217	-3.5
24.98	219	194	-11.3	209	-4.8
31.13	205	184	-10.2	196	-4.3
37.23	186	170	-8.6	180	-3.3
43.29	165	154	-6.7	161	-2.5
49.28	140	136	-2.8	142	-1.4
55.20	120	117	-2.5	122	1.6
61.05	98.2	98.5	0.3	102.6	4.4
66.82	79.9	81.0	1.4	84.2	5.2
72.50	64.7	64.8	0.2	67.4	4.1
78.09	48.8	50.4	3.2	52.3	7.0
83.58	37.0	38.1	3.0	39.4	6.5
88.96	27.1	27.8	2.6	28.7	5.9
96.31	16.7	17.2	3.1	17.4	4.1
103.46	10.4	10.7	2.9	10.6	1.9
110.38	7.57	7.74	2.3	7.50	-0.9
117.08	7.64	7.84	2.6	7.47	-2.2
123.58	10.2	10.3	1.0	9.90	-2.9
132.49	16.0	16.6	3.7	16.2	1.2
141.06	23.1	24.5	5.8	24.3	5.2
145.20	27.5	28.6	4.0	28.5	3.5
149.28	31.2	32.7	4.8	32.6	4.5
157.22	39.3	39.9	1.5	40.1	2.0
164.96	45.4	45.6	4.4	45.9	1.1
168.01	45.9	47.3	3.0	47.6	3.7

It is of interest to compare these results with the more complete angular distribution at 17.45 Mev. The comparison is made two ways. First, phase shifts interpolated between the 17 Mev and 18 Mev solutions described above were used to calculate a cross section, and second an *S* and *P* least-squares analysis was made on the 17.45-Mev data. In this latter calculation, however, it was not possible to fit all angles at once because the code written for the calculating machine would handle only ten angles at a time. Consequently, the 33 angles of that experiment were split into four groups of ten spaced more or less evenly through the range of angles (some angles being repeated in some of the calculations) and the least-squares procedure was carried out on each group. The resulting four sets of phase shifts were averaged and a cross section was computed for the averaged values. The results are listed in Table IV. Here, along with the experimental cross section, are given in the columns labeled I the interpolated phase shifts, the cross section calculated from them, and the percent deviation from the experimental cross section, and in the columns labeled II the averaged phase shifts fitting the 17.45-Mev data with calculated cross section and deviations.

It is seen that in the range of angles below those of

the present experiment, the fit with set I of the phase shifts is particularly poor while set II, though giving a better over-all fit does not agree very well in certain other regions. In the first case it appears that the data suffer from the lack of measurements at forward angles leaving set II more acceptable. On the other hand, the strong systematic deviations in the fit of set II suggest that higher order partial waves are necessary. However, from considerations similar to those mentioned earlier it appears unlikely that *D* phase shifts exceed  $10^\circ$  in magnitude. The averaged phase shifts, set II, are also plotted in Fig. 2 at 17.45 Mev. A line through those points lying more or less parallel to those drawn and connecting with the lower energy phase shifts would give values that are probably within  $\pm 10^\circ$  of being correct.

Once phase shifts are known, the polarization of protons to be expected in proton-helium scattering may be calculated. For phase shifts along the lines in Fig. 2 the polarization at the center-of-mass angle of  $78^\circ$  has a value of  $+70\%$ <sup>23</sup> at 11 Mev and decreases monotonically to a value of  $+57\%$  at 15.5 Mev.

In polarization experiments currently in progress by the author, polarizations of this magnitude and energy variation have been observed at this scattering angle. Also polarizations of the order of the calculated values of  $+20\%$  and  $-94\%$  have been observed at the center-of-mass angles  $37^\circ$  and  $128^\circ$ , respectively. At the present, the measurements are not sufficiently definite to state more than that a rough agreement exists; however, this agreement indicates that there is probably no very large variation of the *D* phase shifts in this energy region. A complete discussion of the polarization experiments and their results is intended for a later paper.

It has come to our attention that least-squares fits to the 17.45-Mev data including *D* waves have been recently made at Los Alamos.<sup>24</sup> Four sets of possible phase shifts were found, one of which agrees roughly with the phase shifts and polarizations reported here. These results are surely the best solution to the problem and the work described in this paper can serve as an aid to extrapolation to the more exact lower energy work. It is of interest that the *D* phase shifts found were of the order of  $10^\circ$ .

I would like to thank Mr. Ezra Shahn for his assistance during the running of the experiment and for his help with some of the tedious desk calculations, and Mrs. Mary Ann Brockman who programmed and assisted in running the least-squares procedure on the IBM 650. The machine calculation was carried out by using the facilities of the IBM Service Bureau Corporation in New York City.

<sup>23</sup> The sign of the polarization here agrees with that given by Critchfield and Dodder (reference 9). It is positive if the polarization vector is in the direction of  $\mathbf{k}_{scatt} \times \mathbf{k}_{inc}$ , where  $\mathbf{k}_{scatt}$  and  $\mathbf{k}_{inc}$  are the scattered and incident wave vectors.

<sup>24</sup> R. M. Thaler and J. L. Gammel (private communication).